

**This item is the archived peer-reviewed author-version of:**

Engineering of hollow periodic mesoporous organosilica nanorods for augmented hydrogen clathrate formation

**Reference:**

Watson Geert, Kummamuru Nithin Bharadwaj, Verbruggen Sammy, Perreault Patrice, Houlleberghs Maarten, Martens Johan, Breynaert Eric, Van Der Voort Pascal.- Engineering of hollow periodic mesoporous organosilica nanorods for augmented hydrogen clathrate formation  
Journal of materials chemistry A : materials for energy and sustainability / Royal Society of Chemistry [London] - ISSN 2050-7496 - 11:47(2023), p. 26265-26276  
Full text (Publisher's DOI): <https://doi.org/10.1039/D3TA05530B>  
To cite this reference: <https://hdl.handle.net/10067/2010070151162165141>

# Journal of Materials Chemistry A

Materials for energy and sustainability

Accepted Manuscript

This article can be cited before page numbers have been issued, to do this please use: G. Watson, N. Kummamuru, S. W. Verbruggen, P. Perreault, M. Houleberghs, J. Martens, E. Breyngaert and P. Van Der Voort, *J. Mater. Chem. A*, 2023, DOI: 10.1039/D3TA05530B.



This is an Accepted Manuscript, which has been through the Royal Society of Chemistry peer review process and has been accepted for publication.

Accepted Manuscripts are published online shortly after acceptance, before technical editing, formatting and proof reading. Using this free service, authors can make their results available to the community, in citable form, before we publish the edited article. We will replace this Accepted Manuscript with the edited and formatted Advance Article as soon as it is available.

You can find more information about Accepted Manuscripts in the [Information for Authors](#).

Please note that technical editing may introduce minor changes to the text and/or graphics, which may alter content. The journal's standard [Terms & Conditions](#) and the [Ethical guidelines](#) still apply. In no event shall the Royal Society of Chemistry be held responsible for any errors or omissions in this Accepted Manuscript or any consequences arising from the use of any information it contains.

# Engineering of Hollow Periodic Mesoporous Organosilica Nanorods for Augmented Hydrogen Clathrate Formation

Geert Watson <sup>a, 1</sup>, Nithin B. Kummamuru <sup>b, 1</sup>, Sammy W. Verbruggen <sup>b, c</sup>,  
Patrice Perreault <sup>d, e</sup>, Maarten Houleberghs <sup>f</sup>, Johan Martens <sup>f</sup>, Eric Breynaert <sup>f</sup>, Pascal Van Der Voort <sup>a, \*</sup>

<sup>a</sup> Centre for Ordered Materials, Organometallics and Catalysis (COMOC), Department of Chemistry, Ghent University, Krijgslaan 281-S3, 9000 Ghent, Belgium.

<sup>b</sup> Sustainable Energy Air & Water Technology (DuEL), Department of Bioscience Engineering, University of Antwerp, Groenenborgerlaan 171, 2020 Antwerpen, Belgium.

<sup>c</sup> NANOLab Center of Excellence, University of Antwerp, Groenenborgerlaan 171, 2020 Antwerpen, Belgium.

<sup>d</sup> Faculty of Science, Instituut voor Milieu & Duurzame Ontwikkeling (IMDO), Campus Groenenborger – Building V.612, Groenenborgerlaan 171, 2020 Antwerpen, Belgium.

<sup>e</sup> University of Antwerp, BlueApp, Olieweg 97, 2020 Antwerpen, Belgium.

View Article Online  
DOI: 10.1039/D3TA05530B

<sup>f</sup> Centre for Surface Chemistry and Catalysis, NMRCoRe - NMR - XRAY - EM Platform for Convergence Research, Department of Microbial and Molecular Systems (M2S), KU Leuven, Celestijnenlaan 200F, 3001, Leuven, Belgium.

\* Corresponding author. E-mail address: [pascal.vandervoort@ugent.be](mailto:pascal.vandervoort@ugent.be)

<sup>1</sup> Contributed equally to this work.

## ABSTRACT

Hydrogen (H<sub>2</sub>) storage, in the form of clathrate hydrates, has emerged as an attractive alternative to classical storage methods like compression or liquefaction. Nevertheless, the sluggish enclathration kinetics along with low gas storage capacities in bulk systems is currently impeding the progress of this technology. To this end, unstirred systems coupled with porous materials have been shown to tackle the aforementioned drawbacks. In line with this approach, the present study explores the use of hydrophobic periodic organosilica nanoparticles, later denoted as Hollow Ring-PMO (HRPMO), for H<sub>2</sub> storage as clathrate hydrates at mild operating conditions (5.56 mol% THF, 7 MPa, and 265-273 K). The surface of the HRPMO nanoparticles was carefully decorated/functionalized with THF-like moieties,

which are well-known promoter agents in clathrate formation when applied in classical, homogeneous systems. The study showed that, while the non-functionalized HRPMO can facilitate the formation of binary H<sub>2</sub>-THF clathrates, the incorporation of surface-bound promoter structures enhances this process. More intriguingly, tuning the concentration of these surface-bound promoter agents on the HRPMO led to a notable effect on solid-state H<sub>2</sub> storage capacities. An increase of 3% in H<sub>2</sub> storage capacity, equivalent to 0.26 wt.%, along with a substantial increase of up to 28% in clathrate growth kinetics, was observed when an optimal loading of 0.14 mmol/g of promoter agent was integrated into the HRPMO framework. Overall, the findings from this study highlight that such tuning effects in solid-state have the potential to significantly boost hydrate formation/growth kinetics and H<sub>2</sub> storage capacities, thereby opening new avenues for the ongoing development of H<sub>2</sub> clathrates in industrial applications.

**KEYWORDS:** Hydrogen storage, Hydrogen clathrates, Hydrophobic porous solids, Promoters, Tetrahydrofuran (THF), Solid state tuning.

## 1. Introduction

While global energy demands are ever-increasing, the extraction and transport of fossil fuels have become progressively more taxing on the environment. On top of this, these resources are finite, so it is of vital importance that a transition to cleaner and more sustainable energy sources is made. Hydrogen ( $H_2$ ), which is clean, carbon neutral, if produced from renewable resources, and has about 2.5 times more calorific value than fossil fuels is increasingly being seen as a crucial pillar of energy security for the associated governments/nations[1, 2]. This is evidenced by  $H_2$  demand climbing 4% in 2022 from pre-pandemic levels of 91 million tonnes in 2019 to an estimated 180 million tonnes by 2030[3]. Given the significant use of  $H_2$  now and in the coming decades, safety and suitability in storage and transportation are essential, however, these are the main limitations impeding the transition of innovative  $H_2$  technologies from production to mobility or energy applications.

$H_2$ , by virtue of its low density (0.08 g/l) requires a large volume for a given amount of energy and the classical  $H_2$  storage approach in its molecular form includes compression, liquefaction, and cryo-compressed technologies[4]. Although these are the more established and mature technologies, they have a variety of drawbacks, such as expensive vessel costs to maintain high pressures (20-70 MPa), heaviness and bulkiness of gas cylinders, higher safety standards, high liquefaction energies, and boil-off losses up to 4% a day[5-8]. Other storage

solutions, such as Adsorption[9-15], Metal hydrides[16-22], Liquid Organic Hydrogen Carriers (LOHC)[23], Ammonia[24], etc., have been proposed in addition to these conventional methods, and tremendous research on these materials is actively being developed in pursuit of better H<sub>2</sub> storage capacities to confront their sluggish kinetics, poor reversibility, cycling instability, and thermal management issues[1, 25-28].

Aside from the above-mentioned H<sub>2</sub> storage systems, hydrate/clathrate based (trapping H<sub>2</sub> in hydrate cages) technology is relatively new and promising, attracting significant interest owing to its advantages. Essentially, trapping H<sub>2</sub> in hydrate cages is environmentally favorable as water (H<sub>2</sub>O) is the principal storage medium, with extremely low concentrations of the promoter molecules (< 6 mol%) if incorporated[29-31]. Second, the stored molecular H<sub>2</sub> can be quickly recovered by pressure or temperature swings with no loss of H<sub>2</sub>O or promoter molecules. Gas hydrates or Clathrate hydrates, are ice-like crystalline materials formed under favorable thermodynamic conditions when suitable guest (usually apolar) molecules are trapped/encaged within the 3-dimensional H<sub>2</sub> bonded host (H<sub>2</sub>O) molecules[32]. Pure H<sub>2</sub> forms a classical sII hydrate structure with 136 H<sub>2</sub>O molecules having a skeleton of sixteen dodecahedron (small) and eight hexakaidecahedron (large) cages between 0.75 and 3.1 GPa at 295 K[33]. Although multiple H<sub>2</sub> occupancy in small and large cages enhances storage

capacity, the pressures mentioned above render them undesirable for any commercial or industrial applications[30, 34-36]. In order to make it industrially viable, incorporating a promoter molecule (tetrahydrofuran: THF) within the large cages, resulting in a binary H<sub>2</sub>-THF hydrate, demonstrated a substantial advancement in H<sub>2</sub> storage via hydrates at pressures as low as 5 MPa and 279.6 K[31]. Despite a tremendous reduction in pressure conditions, the addition of promoter molecules results in a low overall H<sub>2</sub> storage capacity as they occupy large cages and leave only small ones for H<sub>2</sub>. Nevertheless, Lee et al.[37] and other researchers[38] reported to overcome this barrier by tuning the THF concentration from the stoichiometric value of 5.56 mol% to a significantly lower value of 0.15 mol%, allowing H<sub>2</sub> to penetrate some of the large cages. Conversely, many other researchers argue that the H<sub>2</sub> storage is independent of the THF concentration and was unable to replicate equivalent storage capacities by tuning [39-42].

These groundbreaking and contentious findings paved the way for various strategies to improve H<sub>2</sub> storage via hydrate technology at moderate pressures and temperatures. Although significant studies have gained insights into the cage occupancies, overall storage capacities, and thermodynamics with various promoters (THF being reported as the best promoter thus far)[43-45], the authors believe that the constraints on mass transfer rate and enclathration

View Article Online  
DOI: 10.1039/C3JA005530B



kinetics have largely been overlooked, which is a significant impediment to foster this technology. The formation of hydrates from the bulk aqueous phase, in particular, is associated with a slow  $H_2$  uptake rate due to insufficient contact/interaction between  $H_2$  and  $H_2O$  or  $H_2O$  + promoter molecules, which can take up to a few hours or week to reach its maximal storage capacity[37, 40, 46, 47] and mechanical mixing which has the potential to accelerate the kinetics, has major limitations including high energy costs for stirring[48-50]. Other studies attempted to improve the mass diffusion by exposing the high pressure  $H_2$  gas to pre-synthesized fine ( $< 45\mu m$  and  $250\mu m$ ) THF-hydrate, however, this method is not compatible with continuous cycles as fine THF or other promoter hydrate particles relapse to bulk/liquid phase upon melting[40, 46, 51-53]. Given the challenges of synthesizing a binary  $H_2$ -THF hydrate from a bulk aqueous phase, it is imperative to emphasize on quiescent or unstirred systems that would provide accelerated kinetics in developing an efficient and cost-effective  $H_2$  based technology. So far it is evident from the literature that decreasing the particle size or increasing the surface-to-volume ratio enhances the hydrate growth kinetics; however, there has been limited research available on boosting the kinetics of binary  $H_2$ -THF hydrates in an unstirred system packed with porous support materials[39, 51, 54-58]. It is important to note that when exploiting porous materials, multiple variables might contribute significantly to

hydrate formation and kinetics such as pore volume, size, and network for gas saturation at the interface, surface chemistry, and wettability. Contemporary work has shown that hydrophobic porous materials are more efficient than hydrophilic porous materials as H<sub>2</sub>O molecules thermodynamically prefer to minimize their free energy by clustering near the hydrophobic surfaces which amplifies their mobility to promote hydrate nucleation and growth[57-68] and as recently shown for CH<sub>4</sub> clathrate supporting clathrate hydrates with porous materials could dramatically improve the kinetics of gas uptake and release[69].

Considering the superiority of hydrophobicity, the present study attempts to design and develop such a porous material paving the pathway for faster enclathration kinetics of binary H<sub>2</sub> hydrates. Unlike activated carbons, having low dimensional pore networks, this study focuses on periodic mesoporous organosilicas (PMOs) that are carefully architected in terms of pore sizes, network and are additionally functionalized with a highly mobile promoter molecule, THF (thanks to its extended ether chain linking the surface) to investigate their affinity towards forming H<sub>2</sub> hydrate with and without their use in the aqueous phase. Accordingly, the kinetics of binary H<sub>2</sub>-THF hydrate formation and H<sub>2</sub> gas uptake are evaluated by exploiting the porous materials at 265 K, 269 K, and 273 K with an initial pressure of 7 MPa.

View Article Online  
DOI: 10.1039/C3JA05530B

## 2. Experimental methods

### 2.1 Materials synthesis

Cetylammoniumbromide (CTAB),  $\text{NH}_3(\text{aq})$  (25%), ethanol (EtOH),  $\text{HCl}_{\text{aq}}$  (37%), and tetraethyl orthosilicate (TEOS) were purchased from ChemLab. Pluronic F-127 was purchased from Merck Life Science. The organosilanes 1,1,3,3,5,5-hexaethoxy-1,3,5-trisilacyclohexane (HETSCH) and tetrahydrofurfuryloxypropyltriethoxysilane (THFP TES) were purchased from Gelest. All chemicals were used without any additional purification.

Hollow ring PMO (HRPMO) materials with a variation of the added amount of THF-like functionalities were prepared as candidates for the  $\text{H}_2$ -THF clathrate formation. Their synthesis is based on our earlier reported work[70]. In a typical synthesis, a closed flask of 500 ml was charged with 290 ml (16 mol)  $\text{H}_2\text{O}$ , 3 g (8.23 mmol) CTAB, 1.23 g (9.76  $\mu\text{mol}$ ) F-127 and 10 ml (0.134 mmol)  $\text{NH}_3$  (aq, 25%). The whole was left to stir at room temperature until a homogeneous solution was formed. After the addition of 3 ml (13.5 mmol) TEOS, the flask was kept for 2 hours under stirring conditions resulting in the formation of a white solution. At the same time, a mixture of HETSCH and THFP TES was made by mixing a variation of volumes of both monomers (Table 1) in a vial using a shaker. This monomer solution was

subsequently added dropwise to the surfactant solution, after which the mixture was continued to be stirred for 2 more hours at room temperature. Afterward, the flask was placed in an oven where the PMO framework is aged for 48 hours at 373 K. Upon cooling down, the white solids were collected through (vacuum) assisted filtration and subsequently washed with water and ethanol. Surfactant removal was achieved by dispersing the collected residue in a flask containing 600 ml ethanol and 7 ml HCl<sub>aq</sub> (37%), and leaving it to stir at room temperature for 24 hours. Upon collection of the solids through (vacuum) assisted filtration, the residue was washed extensively with ethanol until a neutral pH was reached. The solid materials were dried at 393 K under vacuum conditions (< 5 mbar), resulting in the final HR<sub>x</sub>-THF<sub>y</sub>-PMO materials. In this nomenclature, x and y represent the ratio of HETSCH and THFP TES respectively, added to the reaction mixture (Table 1).

## 2.2. Materials characterization methods

Two-dimensional transmission electron microscopy (2D TEM) pictures were taken using a JEOL JEM-1010 TEM instrument operated at 100kV without spherical aberration (Cs) correction. The powder X-ray diffraction (PXRD) pattern was measured with a Bruker D8 Advance with autochanger using Cu K-alpha irradiation with a wavelength ( $\lambda$ ) of 0.154 nm in

a Bragg-Brentano geometry. PXRD diffractograms were determined in the range of  $2\theta$  from 0 to  $20^\circ$  with a step-size of  $0.015^\circ$ . The porosity of the materials was assessed through  $N_2$ -sorption, as performed on a Micromeritics TriStar 3000 analyzer operated at 77 K. Prior to the analyses, the samples were degassed at 393 K for 24 h. Surface areas were determined using the Brunauer-Emmett-Teller (BET) method, while pore radii ( $r_p$ ) were calculated using DFT methods. Total pore volumes ( $V_{tot}$ ) were determined at a relative pressure of  $\frac{P}{P^0} = 0.95$ . A Thermo Nicolet 6700 Fourier Transform IR (FT-IR) spectrometer, attached with a liquid  $N_2$  cooled MCT detector was used to perform FT-IR measurements. The samples were heated to 393 K under vacuum, for 15 min prior to measurement. Thermogravimetric analysis (TGA) was performed using a Netzsch STA 449 F3 Jupiter instrument within a temperature range of 293 – 1173 K under air with a heating rate of 10 K/min

### 2.3. Experimental apparatus and procedure

The schematic layout of the experimental setup is shown in Figure 1. The hydrate formation tests were performed in high pressure stainless steel cylindrical reactor (effective inner volume:  $150\text{ cm}^3$ , designed pressure 34.4 MPa) purchased from Swagelok (316L-50DF4-150). The high pressure reactor was immersed in a mixture of water-ethylene glycol circulating bath (CORIO

CP-1000F, JULABO GmbH, stability:  $\pm 0.03$  K) to maintain the cold and stable temperatures

View Article Online  
DOI: 10.1039/C3JA05530B

inside the reactor which was measured by a K-type thermocouple purchased from Testo SE & Co. KGaA. The pressure in the reactor was monitored using a pressure transmitter (PAA3X-30 MPa; KELLER AG für Druckmesstechnik; a range of 0-30 MPa absolute, with  $\pm 0.01\%$  FS accuracy) for every 1 sec. H<sub>2</sub> gas (99.99% purity) used in this study was supplied by Air Liquide Benelux Industries.

All the tests were performed using a standard approach as presented in earlier publications[71, 72], here we provide a summary of the same. Prior to the starting of experiments, the reactor was thoroughly cleaned with H<sub>2</sub>O and dried to remove any impurities. The experiments commenced by adding a 1:5 ratio[70] of synthesized material (dried overnight at 348 K) to a certain concentration of the THF solution. Subsequently, the reactor was rapidly pressurized (0.2 MPa) and depressurized with H<sub>2</sub> gas at least 10 times to remove any atmospheric gases. Following that, the reactor was immersed in a water-ethylene glycol bath at 298 K and gradually pressurized with H<sub>2</sub> gas to a predetermined initial experimental pressure of 7 MPa. These ambient thermodynamic conditions were chosen to prevent any hydrate formation and sufficient time was provided for the system to stabilize at these conditions before cooling the reactor to the experimental temperature. The experiments were considered to be complete when

no significant pressure drop (0.02 MPa in 30 min) was observed due to the enclathration of H<sub>2</sub>

gas in the hydrate cages. Each in this study was repeated two times.

At any given real-time, the amount of H<sub>2</sub> gas consumed during hydrate formation was quantified using the compressibility factor equation of state as shown in (Eq. 1), the normalized gas uptake ( $NG_t$ , hydrate growth) was quantified using (Eq. 2), the percentage of H<sub>2</sub>O to hydrate conversion is determined by (Eq. 3) and (Eq. 4)

$$\Delta n_{H_2, t} = V_r \left[ \left( \frac{P}{zRT} \right)_{t=0} - \left( \frac{P}{zRT} \right)_t \right] \quad (\text{Eq. 1})$$

$$NG_t = \frac{\Delta n_{H_2, t}}{n_{H_2O}} \quad (\text{moles of } H_2 / \text{moles of } H_2O) \quad (\text{Eq. 2})$$

$$WtH(\%) = \frac{(\Delta n_{H_2, t} + \Delta n_{THF}) \times Hn}{n_{H_2O}} \times 100 \quad (\text{Eq. 3})$$

$$\Delta n_{THF} = \Delta n_{H_2, t} \frac{\text{number of large cages}}{\text{number of small cages}} \quad (\text{Eq. 4})$$

where,  $\Delta n_{H_2,t}$  is the moles of  $H_2$  gas consumed at any given time  $t$ ;  $V_r$  is the reactor's gas-phase volume measured using the helium expansion method[71, 72];  $T$  and  $P$  are the temperature and pressure within the reactor;  $z$  is the compressibility of  $H_2$  gas calculated using the Lemmon-Huber-Leachman correlation[73];  $R$  is the ideal gas constant;  $n_{H_2O}$  is the moles of  $H_2O$  introduced into the reactor;  $n_{THF}$  is the moles of THF consumed for hydrate formation with the assumption that THF occupies only the large cages of classic sII hydrate, and  $Hn$  refers to hydration number, which is considered to be 5.67 in order to comply with other binary  $H_2$ -THF hydrate experiments available in the literature[74].

The  $H_2$  storage capacity relative to the sample's  $H_2O$  content (hydrate storage capacity:  $q_{H_2}^W$ ),  $H_2$  capacity relative to the dry mass of the solid (dry weight storage capacity:  $q_{H_2}^A$ ), and  $H_2$  capacity relative to the total mass of the system (total weight storage capacity:  $q_{H_2}^T$ ), were also evaluated as shown in (Eqs. 5, 6, and 7)

$$q_{H_2}^W(\text{wt.}\%) = \frac{m_{H_2}}{(m_{H_2O} + m_{H_2})} \times 100 \quad (\text{Eq. 5})$$

$$q_{H_2}^A(\text{wt.}\%) = \frac{m_{H_2}}{(m_{solid} + m_{H_2})} \times 100 \quad (\text{Eq. 6})$$



$$q_{H_2}^T(\text{wt.}\%) = \frac{m_{H_2}}{m_{tot}} \times 100$$

View Article Online  
DOI: 10.1039/D3TA05530B  
(Eq. 7)

Here,  $m_{H_2O}$ ,  $m_{solid}$ , and  $m_{H_2}$  are masses of the  $H_2O$ , dried solid in the reactor, and quantity of enclathrated  $H_2$  as calculated from (Eq. 1), respectively. The  $m_{tot}$  in (Eq. 7) refers to the total mass of the system, considering the mass of the dried solid,  $H_2O$ , THF, as well as the enclathrated  $H_2$ .

Another essential representation, the volumetric gas storage capacity ( $\frac{\text{volume of gas at STP}}{\text{volume of hydrate}}$ ) was determined using (Eq. 8)[75]

$$\text{Volumetric } H_2 \text{ storage capacity} \left( \frac{\text{volume of gas at STP}}{\text{volume of hydrate}} \right) = K \times NG_t \quad (\text{Eq. 8})$$

$$K = \frac{v}{\frac{M_{w,hyd}}{(\rho_{hyd} \times n_{wh})}} \quad (\text{Eq. 9})$$

$$M_{w,hyd} = (136 * 18.01) + (8 * 72.11) + (16 * 2.016) \quad (\text{Eq. 10})$$

$$\rho_{hyd} = \frac{M_{w,hyd}}{(A \times \lambda^3)} \quad (\text{Eq. 11})$$

where  $K$  is the proportionality coefficient and is defined as shown in (Eq. 9),  $v$  is the volume of gas at STP conditions ( $22.4 \text{ cm}^3 \text{ mmol}^{-1}$  of gas),  $M_{w, hyd}$  is molecular weight ( $\text{g mol}^{-1}$ ) of sII hydrate relative to the thermodynamic promoter used in this study (THF), which is calculated as shown in (Eq. 10),  $n_{wh}$  is the mole of  $\text{H}_2\text{O}$  per mole of sII hydrate (i.e. 136),  $\rho_{hyd}$  ( $\text{g cm}^{-3}$ ) is the density of hydrate, calculated using (Eq. 11),  $A$  is the Avogadro constant ( $6.023 \times 10^{23} \text{ mol}^{-1}$ )[76] and  $\lambda$  is the lattice parameter ( $17.145 \text{ \AA}$ ), when THF is used as a promoter and pressurized with  $\text{H}_2$  gas[77].

### 3. Results and discussion

#### 3.1. Material characterizations

The porosity of the PMO materials was assessed through  $\text{N}_2$ -sorption and the resulting isotherms of the as-synthesized materials are displayed in Figure 2a. All materials exhibit a type IV isotherm, characteristic of the mesoporous nature of the PMO framework. The observed  $\text{H}_2$  hysteresis loop indicates that cavitation and percolation phenomena are happening during desorption, implying an inkbottle-like shape of the mesopores in the material. Compared to HRPMO, the addition of THF-moieties in the framework initially causes a decrease in surface area by 21% (Table 2, entries 1 and 2). Upon increasing the THF content in the

framework even more, a steady increase in the surface area is observed (Table 2, entries 3 and

4). This can be attributed to the incorporation of randomly organized THFP TES groups in the PMO matrix, which concurrently induces a reduction of the pore sizes of the materials (Figure 2b). These findings are corroborated through means of XRD analysis (Figure 2c) where the characteristic (100) reflection is shifted towards higher values of  $2\theta$ , demonstrating a decrease in the d-spacing of the framework (Table 2). Clear signs of the siliceous nature of the PMO materials can be recognized through FT-IR spectra (Figure 2d), owing to its typical C-H, Si-OH, and Si-O stretch vibrations at  $3000\text{-}2870\text{ cm}^{-1}$ ,  $3700\text{-}3550\text{ cm}^{-1}$ , and  $1150\text{-}1000\text{ cm}^{-1}$  respectively. More careful investigation of the region of  $3000\text{-}2800\text{ cm}^{-1}$  indicates the presence of novel organic structures in the framework, in the form of THF moieties, for the  $\text{HR}_x\text{-THF}_y\text{-PMOs}$ .

Further confirmation of the incorporation of THF-moieties was found through inspection of the TGA profiles, as displayed in Figure S1, which revealed increasing weight losses at 1173 K when larger amounts of THFP TES were added to the reaction mixture (Table 1). Upon inspection of TEM images, it is found that all PMO materials exhibit a tubular morphology with the long and short axis of the tubes ranging from  $1\text{ }\mu\text{m}$  to several 100 nm respectively (Figure S2). Additionally, the tubes are found to be hollow in nature, with wall thicknesses

ranging in the order of 10-30 nm. Coincidentally, when more THFP TES was added to the reaction mixture the walls become thicker as well as more disordered, substantiating the N<sub>2</sub> sorption and XRD results.

View Article Online  
DOI: 10.1039/C3JA005530B

### 3.2. Effect of the framework composition on H<sub>2</sub> storage

To investigate the influence of THF functionalized hydrophobic porous material (HRPMO) on hydrate formation kinetics and H<sub>2</sub> storage capacity, a set of experiments were initially performed on non-functionalized HRPMO with stoichiometric (5.56 mol%) THF solution at temperatures ranging from 265 K to 273 K with an initial pressure of 7.0 MPa. Considering the data available in the literature[78], the equilibrium pressure of H<sub>2</sub>-THF binary hydrate is  $\approx$  0.1 MPa at 277.5 K, implying that the equilibrium pressures at the temperature conditions studied in this work are expected to be less than 0.1 MPa. However, due to the unavailability of phase equilibrium data at the temperatures studied in this work, we limit ourselves to comparing the driving force with 0.1 MPa, thus the experiments performed in this work correspond to having a driving force  $>$  6.9 MPa between equilibrium pressures at corresponding temperatures. Veluswamy and Linga[74] also reported that a driving force  $>$  5 MPa is necessary to form a considerable amount of H<sub>2</sub>-THF binary hydrates. Table 3. summarizes the experimental

conditions, as well as H<sub>2</sub>-THF hydrate formation results for both THF functionalized and non-functionalized HRPMO. To ensure consistency, 0.5 g of material was used in all the experiments.

Gas hydrate formation being an exothermic process, a sudden rise in sample bed temperature (measured by K-type thermocouple; Testo SE & Co. KGaA) was considered to be the onset of hydrate nucleation, followed by hydrate crystal growth, where the pressure drop observed within the reactor due to gas enclathration was translated to H<sub>2</sub> uptake. Figure 3 shows H<sub>2</sub> storage capacity in a non-functionalized HRPMO at 265 K, 269 K, and 273 K. The time zero in Figure 3 and the subsequent gas uptake Figures in this article corresponds to the onset of hydrate crystal formation (observed from the first temperature spike). As can be seen from Figure 3, a maximum H<sub>2</sub> storage capacity ( $q_{H_2}^W$ ) of 0.25 wt.% was achieved at 269 K; corresponding to 22.74 mmol H<sub>2</sub>/mol H<sub>2</sub>O, followed by a decrease in storage capacity as temperature increased. On the other hand, the three gas uptake curves at different temperatures also demonstrate the consistency of hydrate formation with a minor standard deviation. It can also be seen that the H<sub>2</sub> uptake plateaus off at  $\approx$  40 min after nucleation, with 80% of maximum storage capacity achieved in  $\approx$  8 min, 9 min, and 16.5 min at 265 K, 269 K, and 273 K respectively.

Figures 4a, 4b, and 4c exhibit the H<sub>2</sub> storage capacities of THF-like functionalized HRPMO materials at three different temperatures. The hydrate growth curves show good consistency across the board, as seen by minimal standard deviations. As can be observed, the gas uptake curves show a significant increase before it reaches a plateau, and altering the proportion of these functionalities on the HRPMO produced substantial results in H<sub>2</sub> uptake (Table 3), with HR<sub>95</sub>-THF<sub>5</sub>-PMO outperforming HR<sub>80</sub>-THF<sub>20</sub>-PMO followed by HR<sub>50</sub>-THF<sub>50</sub>-PMO at all temperatures studied. For instance, at the lowest temperature of 265 K, HR<sub>95</sub>-THF<sub>5</sub>-PMO attained a maximum H<sub>2</sub> storage capacity of 0.26 wt.%, which is  $\approx$  13.6% and 21% higher than that of HR<sub>80</sub>-THF<sub>20</sub>-PMO and HR<sub>50</sub>-THF<sub>50</sub>-PMO, respectively. These results also imply that higher amounts of THF-like functionalities added to HRPMO induce a reduction of final H<sub>2</sub> uptake. The H<sub>2</sub> storage capacity at different temperatures for respective materials is shown in Figure S3. Another noteworthy effect of the surface chemistry tuning of the materials lies in the time required to form the H<sub>2</sub> clathrates. It was found that the presence of surface-bound THF-like moieties could significantly stimulate clathrate formation, with the effect becoming more pronounced at higher temperatures (Figure 5). A comparison of the clathrate formation performances at 273 K of non-functionalized HRPMO and HR<sub>95</sub>-THF<sub>5</sub>-PMO demonstrates that

View Article Online  
DOI: 10.1039/C3JA05530B

the THF-like moieties could enhance the hydrate growth kinetics (time required to reach 80% of maximum storage capacity) by at least 28%.

Furthermore, Figure 5 shows the H<sub>2</sub> gas uptake (hydrate growth) curves in non-functionalized HRPMO and HR<sub>95</sub>-THF<sub>5</sub>-PMO, and as can be seen, the materials tuned with THF-like functionalities exhibit relatively higher (at least 3%, inclusive of standard deviation) H<sub>2</sub> gas uptake than HRPMO at all temperatures. These findings unequivocally indicate that the solid-state tuning of the material with the promoter (THF) molecule-like functional groups can improve overall H<sub>2</sub> storage capacities rather than tuning the THF concentration in the solution as reported by Lee et al.[37], which is still being debated. To corroborate the suggestion from Lee et al.[37], the non-functionalized HRPMO and HR<sub>95</sub>-THF<sub>5</sub>-PMO were also tested with 0.1 and 0.3 mol% THF solution, however, no clathrate formation was observed at 265 K for a period of 12 hrs. (plotted until corresponding time in Figure 5).

Based on previous literature reports on hydrophobic porous materials for H<sub>2</sub>-THF clathrate formation, a following mechanistic hypothesis could be drawn for the HRPMO and HR<sub>x</sub>-THF<sub>y</sub>-PMO materials. While pristine HRPMO has been demonstrated to be hydrophobic, due to the organic nature of the utilized organosilica monomer[70], it still shows some degree of hydrophilicity due to the presence of Si-OH functionalities throughout the surface. The

integration of THF-like moieties on the surface of the  $\text{HR}_x\text{-THF}_y\text{-PMO}$  on the other hand

View Article Online  
DOI: 10.1039/C3JA05530B

further enhances the hydrophobicity of the porous structure compared to the HRPMO. The degree of surface hydrophobicity has been shown to influence clathrate formation in two major ways[59, 65], as depicted in Figure 6. Hydrophilic surfaces tend to form a structured organization of water molecules near the surface, known as non-freezable water causing high energy requirements to form ice structures. Hydrophobic surfaces tend to perturb the structural organization of the otherwise strongly ordered surface bound water, lowering the energy requirements necessary to reorganize water molecules towards other crystalline structures (Figure 6, left). The second major influence results from the increase in the concentration of adsorbed gas-molecules ( $\text{H}_2$  in this work) on the hydrophobic surface (Figure 6, right). This gas-enriched layer on the surface of the porous medium increases the driving force of clathrate formation, significantly stimulating the formation kinetics.

It is scientifically known that pure  $\text{H}_2\text{-H}_2\text{O}$  forms sII hydrate at extremely high pressures and can yield a maximum  $\text{H}_2$  storage capacity of 5.6 wt.% if both small and large cages occupy 2 and 5  $\text{H}_2$  molecules, respectively[30, 79] (a probable theoretical maximum  $\text{H}_2$  storage capacities in sII hydrate are presented in Table 4). On the other hand, when THF (thermodynamic promoter) is added to  $\text{H}_2\text{O}$  in stoichiometric concentrations, the  $\text{H}_2$  can only



occupy small cages, leaving large cages for THF, resulting in an overall decreased storage capacity of 1.3 wt.%, when occupied by 1 H<sub>2</sub> molecule and 2.5 wt.% when occupied by 2 H<sub>2</sub> molecules. However, as can be seen from Table 5, in an H<sub>2</sub>-promoter (stoichiometric conc.)-H<sub>2</sub>O system at different thermodynamic conditions, the maximum H<sub>2</sub> storage capacity is < 1.3 wt.% indicating that the fractional H<sub>2</sub> occupancy in small cages is less than 1 or not all small (5<sup>12</sup>) cages are filled at those conditions, which on the other hand can be enhanced by increasing the pressure of the system. Table 5 also shows that solid state tuning of the material can improve the H<sub>2</sub> storage capacity by enclathrating more H<sub>2</sub> molecules in 5<sup>12</sup> cages at relatively low pressures as compared to literature. Although powder-THF hydrate shows better H<sub>2</sub> enclathration, it is to be noted that the fine THF hydrate particles relapse to liquid phase upon melting which is not compatible with continuous cycles.

#### 4. Conclusion

H<sub>2</sub> storage in the form of clathrate hydrates, while being an attractive alternative to compression or liquefaction, remains an energy intensive process. Additives such as THF have been extensively applied to reduce the necessary energy input in the form of lowered formation pressures and milder temperatures. Nevertheless, the constraints on mass transfer rate and

enclathration kinetics in bulk systems have been hampering the advancement of this technology. To this end, unstirred systems coupled with hydrophobic porous materials are being explored due to their ease of handling, recyclability, and potential to accelerate the kinetics of hydrate formation. In this study, hydrophobic Hollow Ring-PMO (HRPMO) nanoparticles with a variation in the concentration of surface-bound THF-like moieties were designed as a novel additive for enhanced H<sub>2</sub> clathrate formation. Their performance was assessed under the stoichiometric concentration of THF solution at 7 MPa in a range of different temperatures (265 K, 269 K, and 273 K) using a volumetric approach. The results revealed that THF-functionalized HRPMO significantly accelerated clathrate formation, reducing the time to reach maximum storage capacity by up to 28%, especially at higher temperatures when compared with non-functionalized HRPMO. Despite having lower surface area and pore volume than the non-functionalized HRPMO, a 3% increase in H<sub>2</sub> storage capacity (inclusive of standard deviation) equating to 0.26 wt.% at lower temperature was observed when 0.14 mmol/g of the promoter was incorporated in the framework. A similar trend in H<sub>2</sub> uptake was observed even at other temperatures studied in this work. On the other hand, higher loadings of promoter agent resulted in a considerable reduction in storage capacities. These findings emphasize the significance of tuning the porous materials with THF-

View Article Online  
DOI: 10.1039/C3JA05530B

like moieties for higher gas storage capacities and these findings resemble previously reported cases that expressed the dependence of H<sub>2</sub> storage capacities on the THF concentrations in H<sub>2</sub>-THF binary clathrates. However, to the best of our knowledge, this is the first report where such a solid-state storage capacity tuning effect is observed using solid additives for H<sub>2</sub> clathrate formation. These findings substantiate the importance of carefully fine-tuning the surface chemistry of additives for clathrate formation and help further pave the way towards industrially viable H<sub>2</sub> storage in the form of clathrate hydrates. In conclusion, it is also strongly recommended to undertake a comprehensive molecular-level investigation in order to attain a more profound understanding of the solid-state tuning effects on supporting materials and their role in augmenting H<sub>2</sub> storage capacities.

#### **CRedit authorship contribution statement**

**Geert Watson:** Writing – review & editing, Writing – original draft, Methodology,

Formal analysis, Conceptualization. **Nithin B. Kummamuru:** Writing – review & editing,

Writing – original draft, Methodology, Formal analysis, Conceptualization. **Pascal Van Der**

**Voort:** Writing – review & editing, Supervision, Methodology, Funding acquisition,

Conceptualization. **Sammy W. Verbruggen:** Supervision, Funding acquisition. **Patrice**

**Perreault:** Writing – review & editing, Supervision, Methodology, Funding acquisition,

Conceptualization. **Eric Breynaert**: Review & Editing, Supervision, Funding acquisition, View Article Online  
DOI: 10.1039/C3TA05530B

Conceptualization. **Johan A. Martens**: Review & Editing, Supervision, Funding acquisition,

Conceptualization. **Maarten Houllberghs**: Review & Editing, Funding acquisition,

Conceptualization.

### Acknowledgment

All authors acknowledge VLAIO for Moonshot funding (ARCLATH, n° HBC.2019.0110, ARCLATH2, n° HBC.2021.0254). PVDV acknowledges UGent for BOFBAS2020000401 for the funding of the XRD diffractometer. M.H. acknowledges FWO for an FWO-SB fellowship. NMRCoRe thanks the Flemish government for financial support as International Research Infrastructure (I001321N: Nuclear Magnetic Resonance Spectroscopy Platform for Molecular Water Research) and acknowledges infrastructure funding from the Department EWI via the Hermes Fund (AH.2016.134). J.A.M. acknowledges the European Research Council (ERC) for an Advanced Research Grant under the European Union's Horizon 2020 Research and Innovation Program under grant agreement No. 834134 (WATUSO).

Corresponding author\*

[pascal.vandervoort@ugent.be](mailto:pascal.vandervoort@ugent.be) Tel:

ORCID

### Notes

The authors declare no competing financial interest.

### Supporting Information

The supporting information is available free of charge on the Publications website at DOI:

**Table 1.** Quantity of the added organosilanes in the HR<sub>x</sub>-THF<sub>y</sub>-PMO synthesisView Article Online  
DOI: 10.1039/D3TA05530B

Sample	V <sub>HETSCH</sub> (ml) n <sub>HETSCH</sub> (mmol)	V <sub>THFPTEs</sub> (ml) n <sub>THFPTEs</sub> (mmol)
HRPMO	3	/
	8.24	
HR <sub>95</sub> -THF <sub>5</sub> -PMO	2.85	0.15
	7.83	0.48
HR <sub>80</sub> -THF <sub>20</sub> -PMO	2.4	0.6
	6.59	1.94
HR <sub>50</sub> -THF <sub>50</sub> -PMO	1.5	1.5
	4.12	4.85

**Table 2.** Overview of the characteristics of the PMO materials.

Entry	Sample	THFP TES loading (mmol/g) <sup>a</sup>	$S_{BET}$ (m <sup>2</sup> /g)	$V_{tot}$ (cm <sup>3</sup> /g) <sup>b</sup>	$r_p$ (nm) <sup>c</sup>	d-spacing (nm) <sup>d</sup>
1	HRPMO	/	790	0.90	1.89	5.04
2	HR <sub>95</sub> -THF <sub>5</sub> -PMO	0.14	620	0.56	1.77	5.01
3	HR <sub>80</sub> -THF <sub>20</sub> -PMO	0.48	650	0.85	1.65	4.47
4	HR <sub>50</sub> -THF <sub>50</sub> -PMO	1.11	850	0.71	1.29	3.88

<sup>a</sup> Determined using TGA profiles between 200-900°C; <sup>b</sup> Determined at P/P°=0.95; <sup>c</sup> Determined using a NLDFT method assuming a silica matrix exhibiting cylindrical pores on the adsorption

branch with relative fitting errors <1%; <sup>d</sup> Determined using Bragg's law with  $\lambda=0.154$  nm)

**Table 3.** Summary of H<sub>2</sub> storage capacities in H<sub>2</sub>/THF(5.56 mol%)/H<sub>2</sub>O system in functionalized and non-functionalized HRPMO at different thermodynamic conditions

System	P (MPa)	T (K)	$NG_t$ (moles H <sub>2</sub> /moles H <sub>2</sub> O)	$WtH$ (%)	$q_{H_2}^W$ (wt.%)	$q_{H_2}^A$ (wt.%)	$q_{H_2}^T$ (wt.%)	Volumetric H <sub>2</sub> storage (v/v)
Non-functionalized HRPMO	7	265	22.75	19.35	0.254	1.042	0.205	22.83
	7	269	20.55	17.46	0.229	0.941	0.185	20.61
	7	273	19.38	16.48	0.216	0.889	0.174	19.45
HR <sub>95</sub> -THF <sub>5</sub> -PMO	7	265	23.61	20.08	0.264	1.081	0.212	23.70
	7	269	21.53	18.31	0.240	0.986	0.194	21.61
	7	273	20.08	17.09	0.224	0.921	0.181	20.17
HR <sub>80</sub> -THF <sub>20</sub> -PMO	7	265	20.77	17.68	0.232	0.952	0.187	20.85

	7	269	19.45	16.54	0.217	0.892	0.175	19.53
	7	273	17.51	14.89	0.196	0.804	0.158	17.58
HR <sub>50</sub> -THF <sub>50</sub> -PMO	7	265	19.49	16.59	0.218	0.895	0.176	19.58
	7	269	18.21	15.49	0.203	0.836	0.164	18.28
	7	273	16.52	14.05	0.185	0.759	0.149	16.59



**Table 4.** Theoretical storage capacity of H<sub>2</sub> in sII hydrate cages

System	Small cage (5 <sup>12</sup> )	Large cage (5 <sup>12</sup> 6 <sup>4</sup> )	H <sub>2</sub> storage capacity (wt.%)
H <sub>2</sub> -H <sub>2</sub> O	1	1	1.94
	1	2	2.56
	1	3	3.19
	1	4	3.80
	1	5	4.40
	2	1	3.18
	2	2	3.80
	2	3	4.40
	2	4	5.00
	2	5	5.60
H <sub>2</sub> -THF-H <sub>2</sub> O	1	0	1.30
	2	0	2.56

**Table 5.** H<sub>2</sub> storage capacity in sII hydrates below 15 MPa using promoters (stoichiometric conc.)

View Article Online  
DOI: 10.1039/C3JA005530B

System	P (MPa)	T (K)	H <sub>2</sub> storage capacity (wt.%)	Occupancy of 5 <sup>12</sup> cages* (%)	Ref.
THF in Porous media (HR <sub>95</sub> -THF <sub>5</sub> -PMO)	7.0	265	0.26	10.05	This work
	7.0	269	0.24	9.14	
	7.0	273	0.22	8.37	
THF-Bulk solution/stirring	13	279.2	0.183	6.96	[80]
DIOX-Bulk solution/stirring	12.3	271.15	0.216	8.22	[75]
THF in Porous media	11.6	270	0.4	15.25	[55]
Powdered DXN hydrate	12.0	233	0.4	15.25	[81]
ECP-Bulk solution	12.2	273.25	0.310	11.81	[53]
THF-Bulk solution/stirring	7.0	278.2	0.14	5.25	[74]
	5.0	278.2	0.12	4.40	
	5.0	278.2	0.13	4.76	
	5.0	278.2	0.10	3.92	
Powdered THF hydrate	5.0	265.1	0.18	6.85	[82]
	5.0	269	0.16	6.10	
	5.0	273.2	0.15	5.71	
Powdered THF hydrates	6.5	269.5	0.23	8.75	[83]
	6.5	269.5	0.23	8.75	
	6.5	269.5	0.20	7.61	
	8.4	269.5	0.25	9.52	
	6.5	269.5	0.23	8.75	

	3.6	269.5	0.19	7.23	View Article Online DOI: 10.1039/D3TA05530B
	6.5	266.7	0.26	9.90	
	6.5	269.5	0.23	8.75	
	6.5	275.1	0.21	7.99	
Powdered THF hydrate	6.7	270	0.36	13.63	[40]
	12.2		0.46	17.70	
	6.2		0.38	14.56	
	12.1		0.55	21.13	
	12.4		0.32	12.28	
Powdered THF hydrates	10.7	277.15	0.19	7.23	[52]
	11.4		0.26	9.90	

\*Considering two H<sub>2</sub> molecules in a single small cage

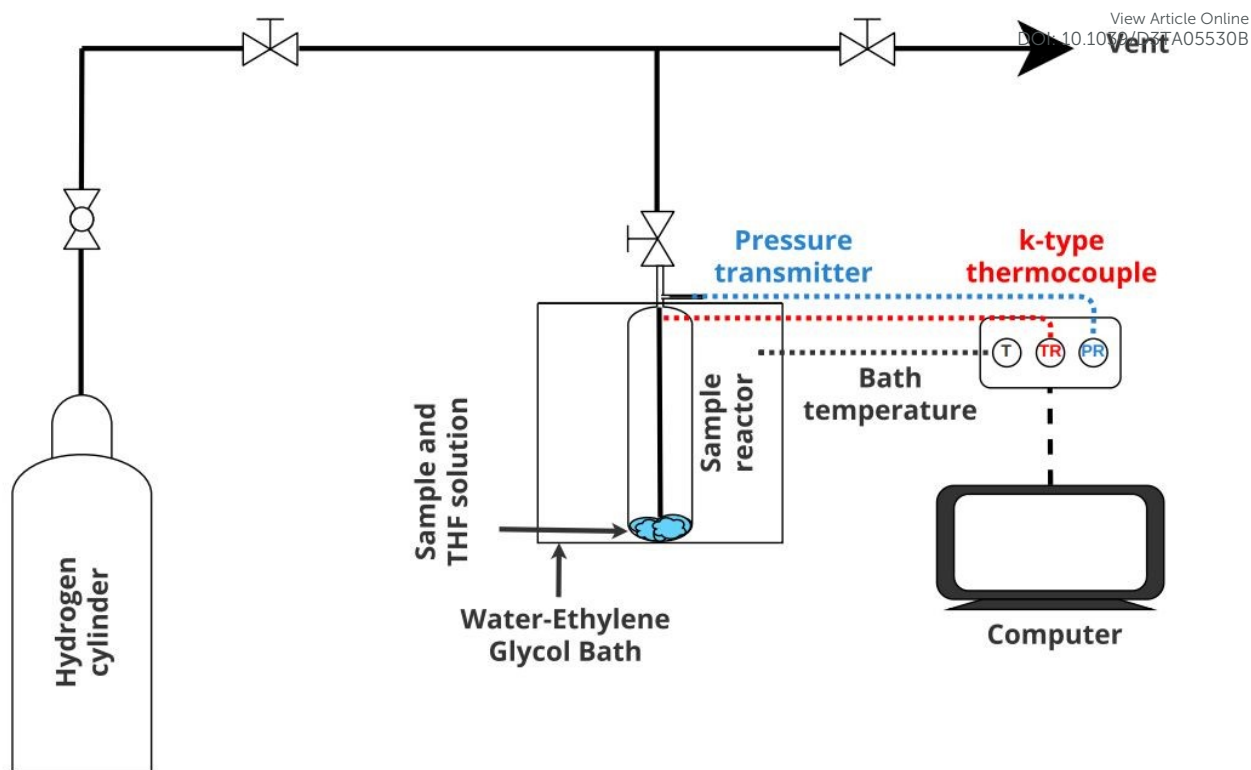


**Figure 1.** The schematic of the experimental setup for the study of binary H<sub>2</sub>-THF hydrate formation in HRPMO

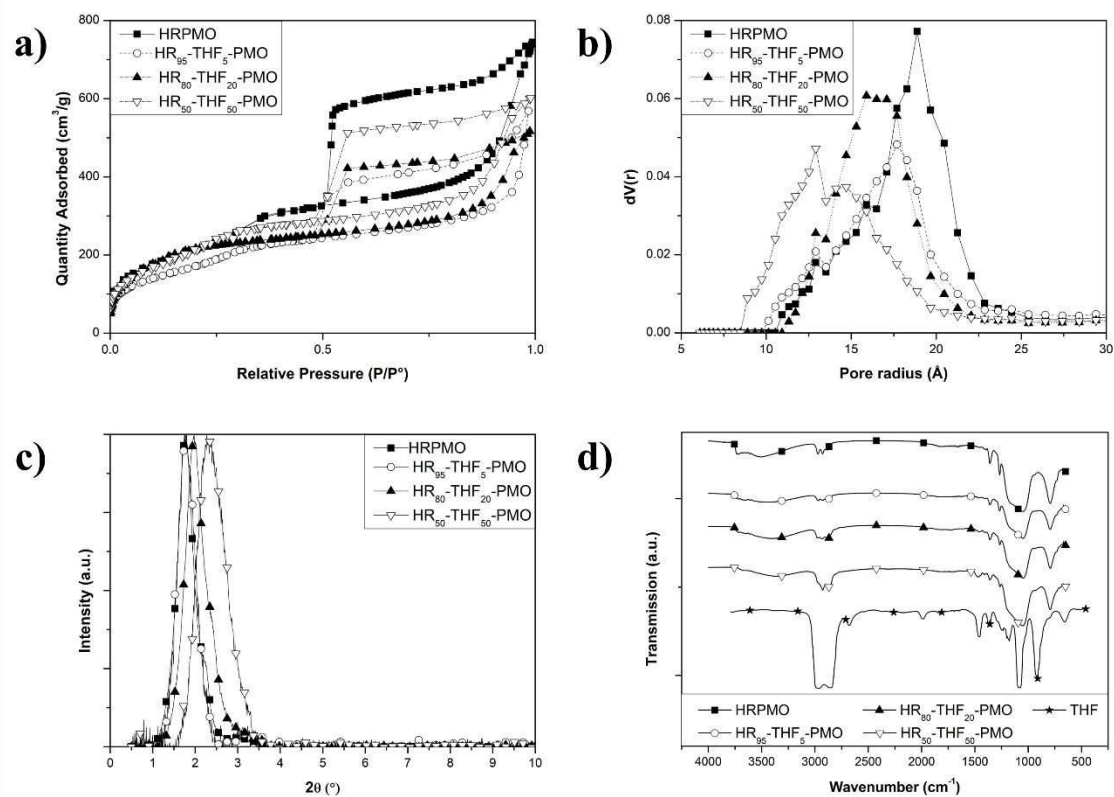


**Figure 2.** Overview of the characteristics of the PMO materials: a) N<sub>2</sub> sorption isotherms, b) DFT calculated pore size distributions, c) XRD diffractograms, d) FTIR spectra.

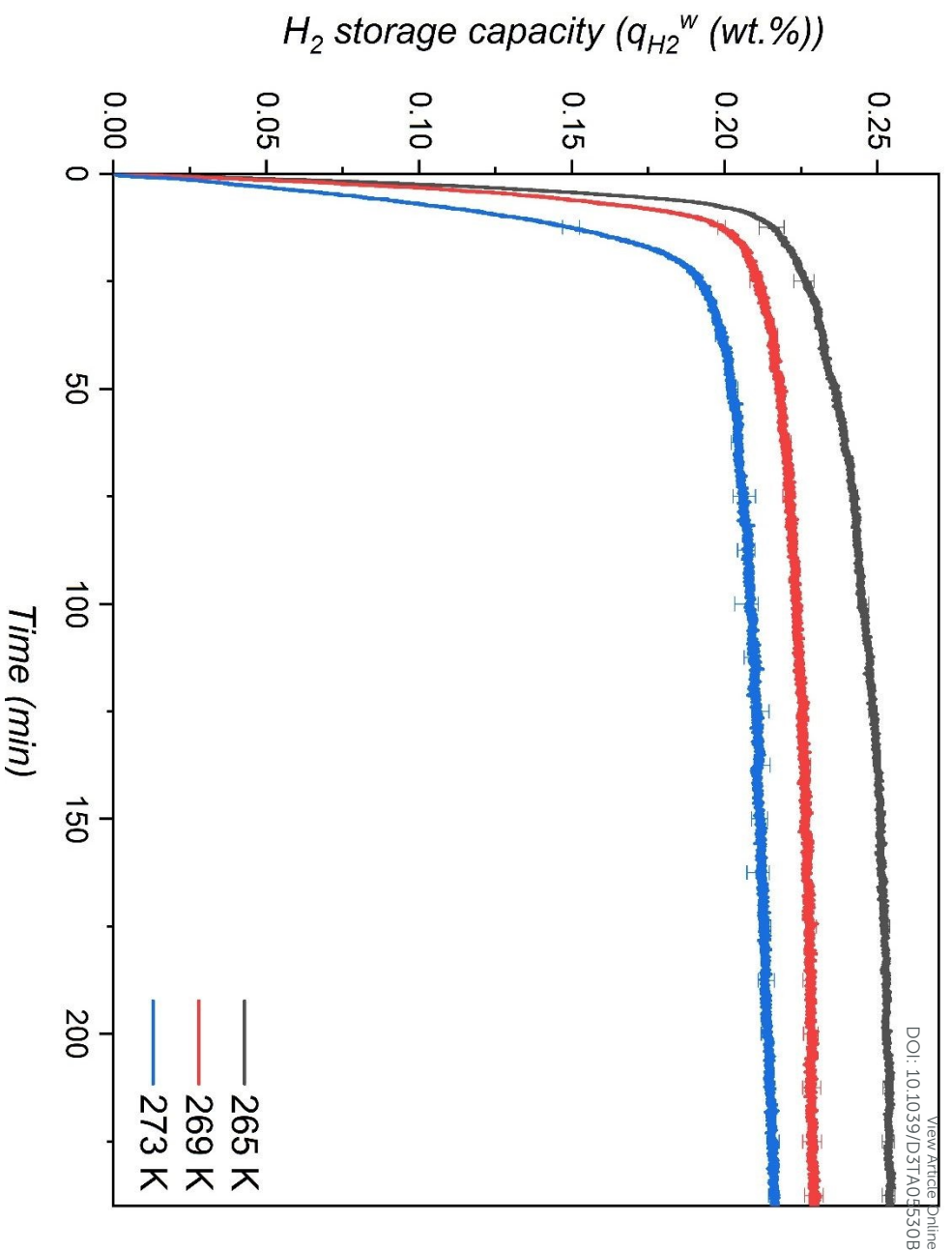
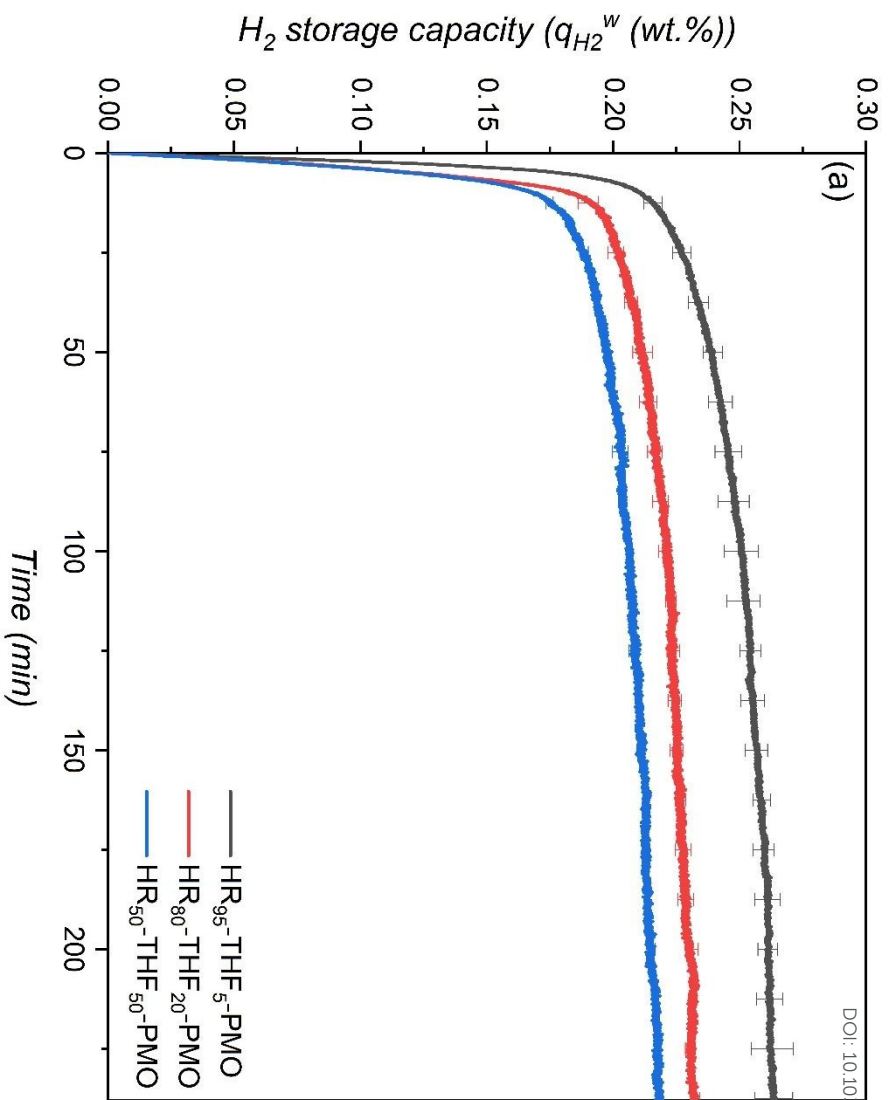
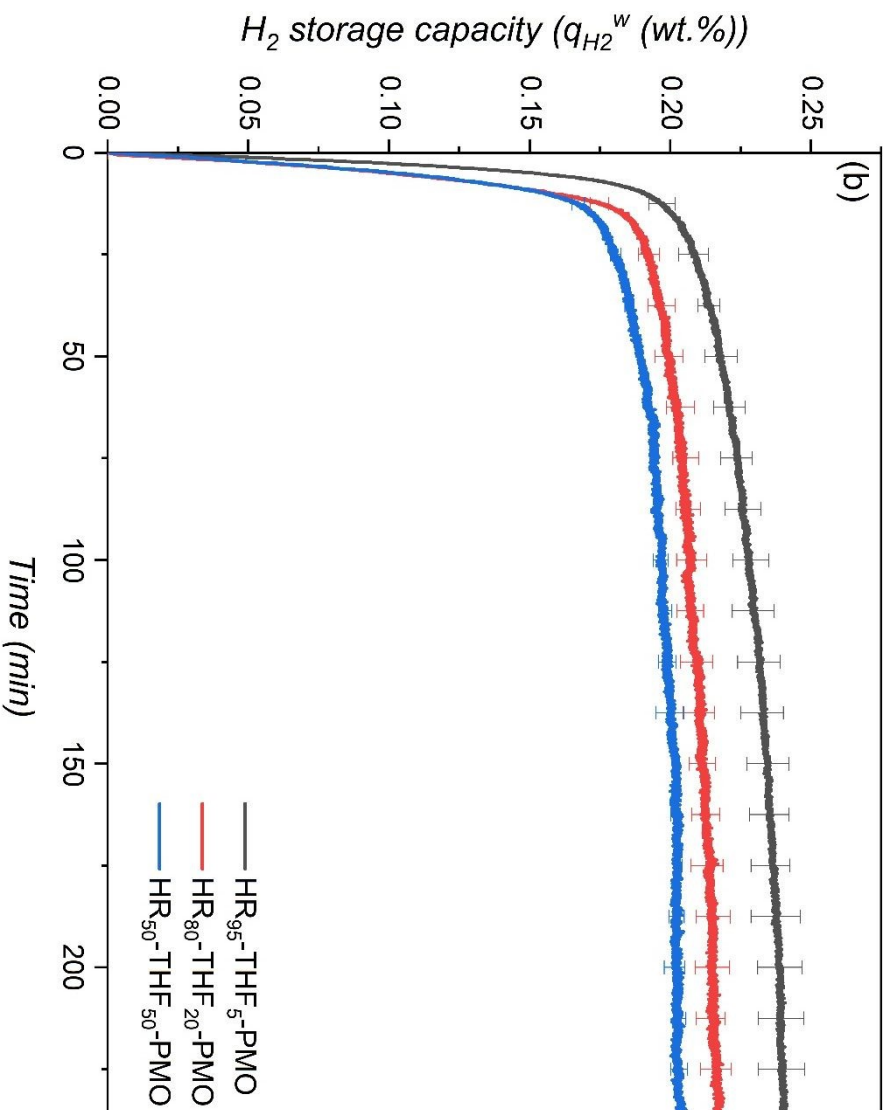
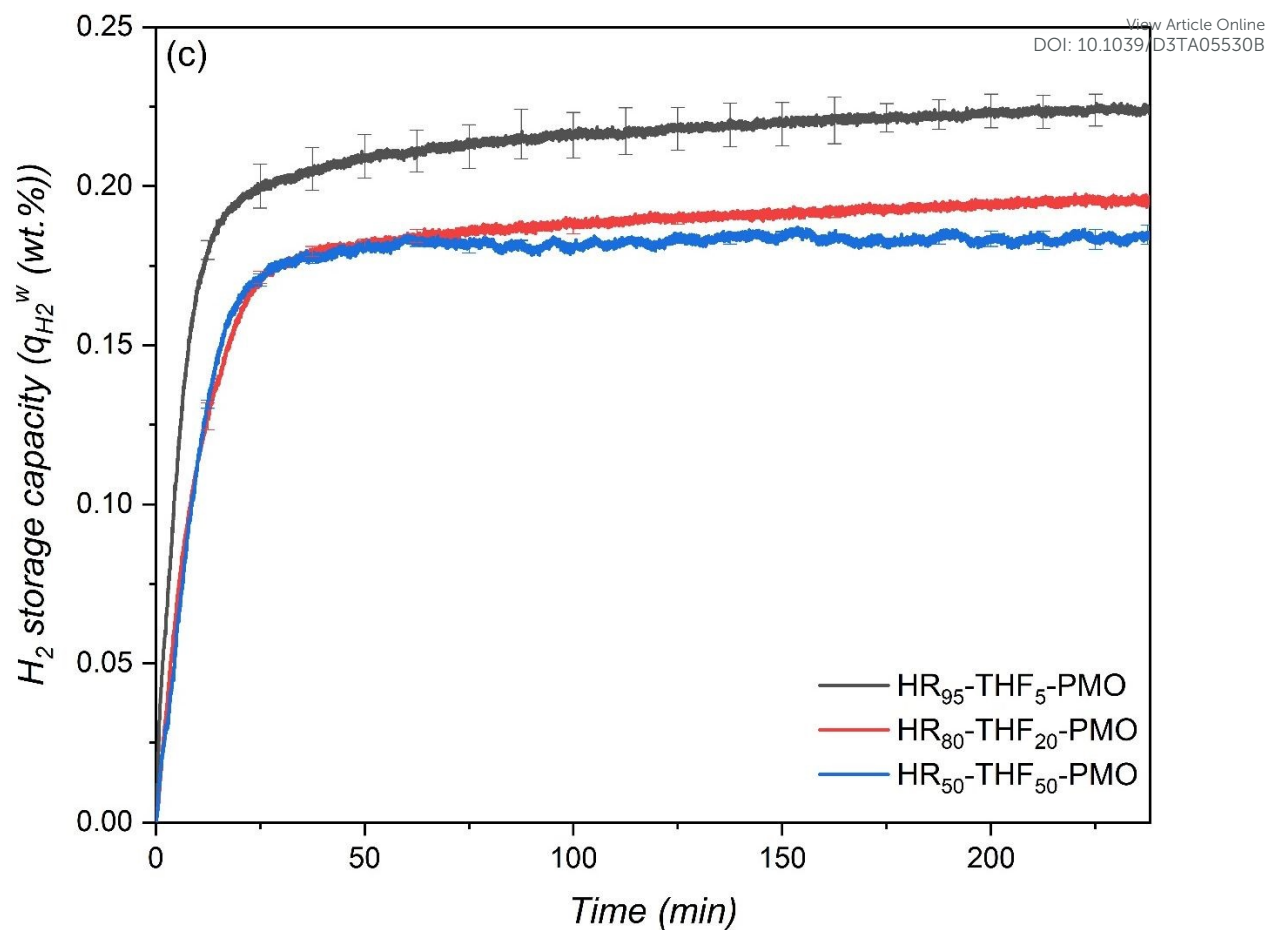


Figure 3.  $H_2$  storage capacity at three different temperatures in non-functionalized HRPiMO

View Article Online  
DOI: 10.1039/D3TA05530B



**Figure 4.** H<sub>2</sub> storage capacities in three different THF-like functionalized materials at three different temperatures; (a): 265 K, (b): 269 K, (c): 273 K



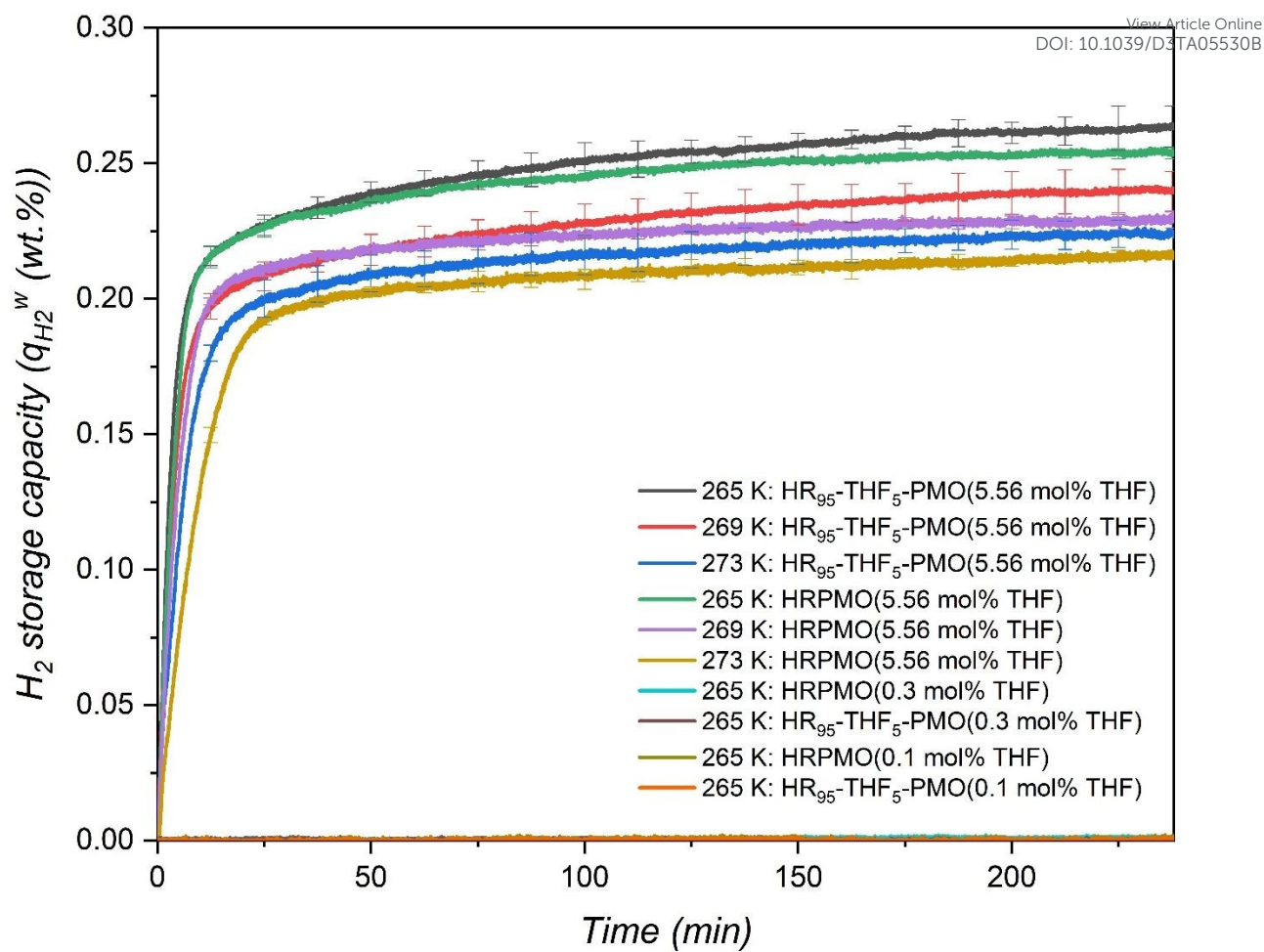


**Figure 5.** H<sub>2</sub> gas uptake (hydrate growth) curves in non-functionalized HRPMO and HR<sub>95</sub>-THF<sub>5</sub>-PMO at different temperatures under 5.56 mol%, 0.1 mol% and 0.3 mol% THF conditions.

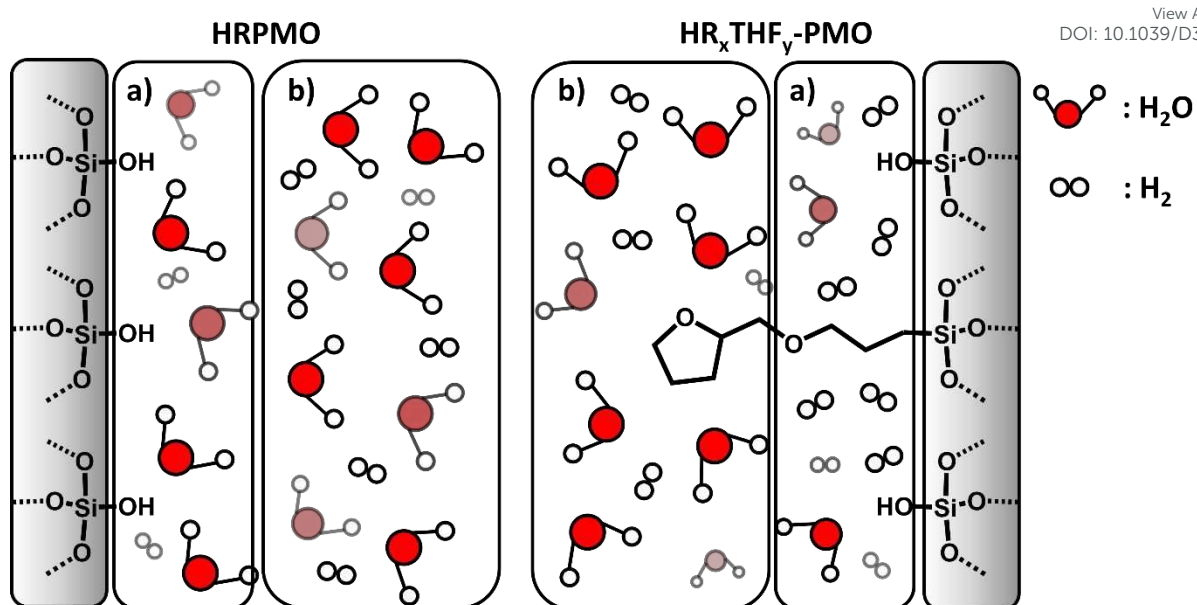


Figure 6: Depiction of differences in clathrate formation in HRP MO (left) versus HR<sub>x</sub>-THF<sub>y</sub>-PMO (right).

## References

- [1] E. Tzimas, C. Filiou, S. D. Peteves, J. B. Veyre, *Hydrogen storage: State-of-the-art and future perspective*, Netherlands, 2003,
- [2] IEA, *Global hydrogen review 2022*, Paris, 2022, <https://www.iea.org/reports/global-hydrogen-review-2022>
- [3] IEA, *Hydrogen*, Paris, 2022, <https://www.iea.org/reports/hydrogen>
- [4] M. Hirscher, *Handbook of hydrogen storage: New materials for future energy storage*, Wiley-VCH Verlag GmbH & Co. KGaA, Weinheim, Germany, 2010.
- [5] H. Barthélémy, M. Weber, F. Barbier, *Hydrogen storage: Recent improvements and industrial perspectives*, *Int. J. Hydrogen Energy* 42 (2017) 7254-7262.
- [6] R. S. Irani, *Hydrogen storage: High-pressure gas containment*, *MRS Bulletin* 27 (2002) 680-682.
- [7] A. Züttel, *Materials for hydrogen storage*, *Mater. Today* 6 (2003) 24-33.
- [8] V. V. Struzhkin, B. Militzer, W. L. Mao, H-K. Mao, R. J. Hemley, *Hydrogen storage in molecular clathrates*, *Chem. Rev.* 107 (2007) 4133-4151.
- [9] M. Mohan, V. K. Sharma, E. A. Kumar, V. Gayathri, *Hydrogen storage in carbon materials—A review*, *Energy storage* 1 (2019) e35.
- [10] D. Zhao, X. Wang, L. Yue, Y. He, B. Chen, *Porous metal–organic frameworks for hydrogen storage*, *Chem. Commun.* 58 (2022) 11059-11078.
- [11] L. Zhang, M. D. Allendorf, R. Balderas-Xicohténcatl, D. P. Broom, G. S. Fanourgakis, G. E. Froudakis, T. Gennett, K. E. Hurst, S. Ling, C. Milanese, P. A. Parilla, D. Pontiroli, M. Riccò, S. Shulda, V. Stavila, T. A. Steriotis, C. J. Webb, M. Witman, M. Hirscher, *Fundamentals of hydrogen storage in nanoporous materials*, *Prog. Energy* 4 (2022) 042013.
- [12] Á. Berenguer-Murcia, J. P. Marco-Lozar, D. Cazorla-Amorós, *Hydrogen storage in porous materials: Status, Milestones, and Challenges*, *Chem. Rec.* 18 (2018) 900-912.
- [13] Z. Chen, K. O. Kirlikovali, K. B. Idrees, M. C. Wasson, O. K. Farha, *Porous materials for hydrogen storage*, *Chem* 8 (2022) 693-716.
- [14] K. M. Thomas, *Hydrogen adsorption and storage on porous materials*, *Catal. Today* 120 (2007) 389-398.
- [15] M. Pumera, *Graphene-based nanomaterials for energy storage*, *Energy Environ. Sci.* 4 (2011) 668-674.

- [16] E. Rivard, M. Trudeau, K. Zaghbi, Hydrogen storage for mobility: A review, *Materials* 19 (2019) 1973. View Article Online  
DOI: 10.1039/C9TA05530B
- [17] N. A. A. Rusman, M. Dahari., A review on the current progress of metal hydrides material for solid-state hydrogen storage applications, *Int. J. Hydrogen Energy* 41 (2016) 12108-12126.
- [18] B. Sakintuna, F. Lamari-Darkrim, M. Hirscher, Metal hydride materials for solid hydrogen storage: A review, *Int. J. Hydrogen Energy* 32 (2007) 1121-1140.
- [19] P. Modi, K. F. Aguey-Zinsou, Room temperature metal hydrides for stationary and heat storage applications: A review, *Front. Energy Res.* 9 (2021).
- [20] J. Graetz, New approaches to hydrogen storage, *Chem. Soc. Rev.* 38 (2009) 73-82.
- [21] F. Schuth, B. Bogdanovic, M. Felderhoff, Light metal hydrides and complex hydrides for hydrogen storage, *Chem. Commun.* (2004) 2249-2258.
- [22] R. B. Biniwale, S. Rayalu, S. Devotta, M. Ichikawa, Chemical hydrides: a solution to high capacity hydrogen storage and supply, *Int. J. Hydrogen Energy* 33 (2008) 360-365.
- [23] C. Chu, K. Wu, B. Luo, Q. Cao, H. Zhang, Hydrogen storage by liquid organic hydrogen carriers: Catalyst, renewable carrier, and technology – A review, *Carbon Resour. Convers.* 6 (2023) 334-351.
- [24] M. Aziz, A. T. Wijayanta, A. B. D. Nandiyanto, Ammonia as Effective Hydrogen Storage: A Review on Production, Storage and Utilization, *Energies* 13 (2020) 3062.
- [25] H. W. Langmi, N. Engelbrecht, P. M. Modisha, D. Bessarabov, Chapter 13 - Hydrogen storage, in: T. Smolinka, J. Garche, (Eds.), *Electrochemical Power Sources: Fundamentals, Systems, and Applications*, Elsevier, 2022, pp. 455-486.
- [26] H. Q. Nguyen, B. Shabani, Review of metal hydride hydrogen storage thermal management for use in the fuel cell systems, *Int. J. Hydrogen Energy* 46 (2021) 31699-31726.
- [27] P. Perreault, L. V. Hoecke, H. Pourfallah, N. B. Kummamuru, C.-R. Boruntea, P. Preuster, Critical challenges towards the commercial rollouts of a LOHC-based H<sub>2</sub> economy, *Curr. Opin. Green Sustain. Chem.* 41 (2023) 100836.
- [28] S. Chatterjee, R. K. Parsapur, K.-W. Huang, Limitations of Ammonia as a Hydrogen Energy Carrier for the Transportation Sector, *ACS Energy Lett.* 6 (2021) 4390-4394.
- [29] Y. A. Dyadin, E. G. Larionov, A. Y. Manakov, F. V. Zhurko, E. Y. Aladko, T. V. Mikina, V. Y. Komarov, Clathrate hydrates of hydrogen and neon, *Mendelev Commun.* 5 (1999) 209-210.

- [30] W. L. Mao, H. K. Mao, A. F. Goncharov, V. V. Struzhkin, Q. Z. Guo, J. Z. Hu, J. D. Shu, M.S. R. J. Hemley, Y. S. Zhao, Hydrogen clusters in clathrate hydrate, *Science* 297 (2002) 2247-2249.
- [31] L. J. Florusse, C. J. Peters, J. Schoonman, K. C. Hester, C. A. Koh, S. F. Dec, K. N. Marsh, E. D. Sloan, Stable low-pressure hydrogen clusters stored in a binary clathrate hydrate, *Science* 306 (2004) 469-471.
- [32] E. D. Sloan, C. A. Koh, Clathrate hydrates of natural gases, 3 ed., Taylor & Francis-CRC Press, Boca Raton, FL, 2008.
- [33] W. L. Vos, L. W. Finger, R. J. Hemley, H-k. Mao, Novel H<sub>2</sub>-H<sub>2</sub>O clathrates at high pressures, *Phys. Rev. Lett.* 71 (1993) 3150-3153.
- [34] Y. A. Dyadin, E. G. Larionov, E. Y. Aladko, A. Y. Manakov, F. V. Zhurko, T. V. Mikina, V. Y. Komarov, E. V. Grachev, Clathrate formation in water-noble gas (hydrogen) systems at high pressures *J. Struct. Chem.* 40 (1999) 790-795.
- [35] K. A. Lokshin, Y. Zhao, D. He, W. L. Mao, H-K. Mao, R. J. Hemley, M. V. Lobanov, M. Greenblatt, Structure and dynamics of hydrogen molecules in the novel clathrate hydrate by high pressure neutron diffraction, *Phys. Rev. Lett.* 93 (2004) 125503.
- [36] S. Patchkovskii, J. S. Tse, Thermodynamic stability of hydrogen clathrates, *PNAS* 100 (2003) 14645-14650.
- [37] H. Lee, J.-W. Lee, D. Y. Kim, J. Park, Y. T. Seo, H. Zeng, I. L. Moudrakovski, C. I. Ratcliffe, J. A. Ripmeester, Tuning clathrate hydrates for hydrogen storage, *Nature* 434 (2005) 743-746.
- [38] D-Y. Kim, Y. Park, H. Lee, Tuning clathrate hydrates: Application to hydrogen storage, *Catal. Today* 120 (2007) 257-261.
- [39] R. Anderson, A. Chapoy, B. Tohidi, Phase relations and binary clathrate hydrate formation in the system H<sub>2</sub>-THF-H<sub>2</sub>O, *Langmuir* 23 (2007) 3440-3444.
- [40] T. A. Strobel, C. J. Taylor, K. C. Hester, S. F. Dec, C. A. Koh, K. T. Miller, E. D. Sloan, Molecular hydrogen storage in binary THF-H<sub>2</sub> clathrate hydrates, *J. Phys. Chem. B* 110 (2006) 17121-17125.
- [41] N. I. Papadimitriou, I. N. Tsimpanogiannis, A. Th. Papaioannou, A. K. Stubos, Evaluation of the hydrogen-storage capacity of pure H<sub>2</sub> and binary H<sub>2</sub>-THF hydrates with monte carlo simulations, *J. Phys. Chem. C* 112 (2008) 10294-10302.
- [42] S. Hashimoto, T. Sugahara, H. Sato, K. Ohgaki, Thermodynamic Stability of H<sub>2</sub> + tetrahydrofuran mixed gas hydrate in nonstoichiometric aqueous solutions, *J. Chem. Eng. Data* 52 (2007) 517-520.

- [43] A. Gupta, G. V. Baron, P. Perreault, S. Lenaerts, R-G. Ciocarlan, P. Cool, P. G. M. Mileo, S. Rogge, V. V. Speybroeck, G. Watson, P. V. D. Voort, M. Houllberghs, E. Breynaert, J. Martens, J. F. M. Denayer, Hydrogen clathrates: Next generation hydrogen storage materials, *Energy Storage Mater.* 41 (2021) 69-107.
- [44] H. P. Veluswamy, R. Kumar, P. Linga, Hydrogen storage in clathrate hydrates: Current state of the art and future directions, *Appl. Energy* 122 (2014) 112-132.
- [45] H. P. Veluswamy, W. J. Ang, D. Zhao, P. Linga, Influence of cationic and non-ionic surfactants on the kinetics of mixed hydrogen/tetrahydrofuran hydrates, *Chem. Eng. Sci.* 132 (2015) 186-199.
- [46] A. Lokshin, Y. Zhao, Fast synthesis method and phase diagram of hydrogen clathrate hydrate, *Appl. Phys. Lett.* 88 (2006) 131909.
- [47] S. Alavi, J. A. Ripmeester, Hydrogen-gas migration through clathrate hydrate cages, *Angew. Chem. Int. Ed.* 46 (2007) 6102-6105.
- [48] P. Englezos, Nucleation and growth of gas hydrate crystals in relation to kinetic inhibition, *Rev IFP* 51 (1996) 789.
- [49] F. Rossi, M. Filipponi, B. Castellani, Investigation on a novel reactor for gas hydrate production, *Appl. Energy* 99 (2012) 167-172.
- [50] A. Vysniauskas, P.R. Bishnoi, A kinetic study of methane hydrate formation, *Chem. Eng. Sci.* 38 (1983) 1061-1072.
- [51] A. Talyzin, Feasibility of H<sub>2</sub>-THF-H<sub>2</sub>O clathrate hydrates for hydrogen storage applications, *Int. J. Hydrogen Energy* 33 (2008) 111-115.
- [52] K. Ogata, S. Hashimoto, T. Sugahara, M. Moritoki, H. Sato, K. Ohgaki, Storage capacity of hydrogen in tetrahydrofuran hydrate, *Chem. Eng. Sci.* 63 (2008) 5714-5718.
- [53] S. Chen, Y. Wang, X. Lang, S. Fan, G. Li, Rapid and high hydrogen storage in epoxycyclopentane hydrate at moderate pressure, *Energy* 268 (2023) 126638.
- [54] F. Su, C. L. Bray, B. O. Carter, G. Overend, C. Cropper, J. A. Iggo, Y. Z. Khimyak, A. M. Fogg, A.I. Cooper, Reversible hydrogen storage in hydrogel clathrate hydrates, *Adv. Mater.* 21 (2009) 2382-2386.
- [55] F. Su, C. L. Bray, B. Tan, A. I. Cooper, Rapid and reversible hydrogen storage in clathrate hydrates using emulsion-templated polymers, *Adv. Mater.* 20 (2008) 2663-2666.
- [56] D. Saha, S. Deng, Accelerated Formation of THF-H<sub>2</sub> Clathrate Hydrate in Porous Media, *Langmuir* 26 (2010) 8414-8418.

View Article Online  
DOI: 10.1039/C3TA05530B

- [57] D. Saha, S. Deng, Enhanced hydrogen adsorption in ordered mesoporous carbon through clathrate formation, *Int. J. Hydrogen Energy* 34 (2009) 8583-8588.
- [58] J. Farrando-Perez, R. Balderas-Xicohtencatl, Y. Cheng, L. Daemen, C. Cuadrado-Collados, M. Martinez-Escandell, A. J. Ramirez-Cuesta, J. Silvestre-Albero, Rapid and efficient hydrogen clathrate hydrate formation in confined nanospace, *Nature* 13 (2022) 5953.
- [59] M. E. Casco, E. Zhang, S. Grätz, S. Krause, V. Bon, D. Wallacher, N. Grimm, D. M. Többens, T. Hauß, L. Borchardt, Experimental evidence of confined methane hydrate in hydrophilic and hydrophobic model carbons, *J. Phys. Chem. C* 123 (2019) 24071-24079.
- [60] M. E. Casco, J. S. Albero, A. J. Ramírez-Cuesta, F. Rey, J. L. Jordá, A. Bansode, A. Urakawa, I. Peral, M. M. Escandell, K. Kaneko, F. R. Reinoso, Methane hydrate formation in confined nanospace can surpass nature, *Nat. Commun.* 6 (2015) 6432.
- [61] N. N. Nguyen, A. V. Nguyen, Hydrophobic effect on gas hydrate formation in the presence of additives, *Energy Fuels* 31 (2017) 10311-10323.
- [62] M. S. P. Sansom, P. C. Biggin, Water at the nanoscale, *Nature* 414 (2001) 157-159.
- [63] Z. Li, R.-H. Yoon, Thermodynamics of hydrophobic interaction between silica surfaces coated with octadecyltrichlorosilane, *J. Colloid Interface Sci.* 392 (2013).
- [64] J. Miyawaki, T. Kanda, T. Suzuki, T. Okui, Y. Maeda, K. Kaneko, Macroscopic evidence of enhanced formation of methane nanohydrates in hydrophobic nanospaces, *J. Phys. Chem. B* 102 (1998) 2187-2192.
- [65] N. N. Nguyen, A. V. Nguyen, K. M. Steel, L. X. Dang, M. Galib, Interfacial gas enrichment at hydrophobic surfaces and the origin of promotion of gas hydrate formation by hydrophobic solid particles, *J. Phys. Chem. C* 121 (2017) 3830-3840.
- [66] H. Li, L. Wang, Hydrophobized particles can accelerate nucleation of clathrate hydrates, *Fuel* 140 (2015) 440-445.
- [67] N. N. Nguyen, M. Galib, A. V. Nguyen, Critical Review on Gas Hydrate Formation at Solid Surfaces and in Confined Spaces-Why and How Does Interfacial Regime Matter?, *Energy Fuels* 34 (2020) 6751-6760.
- [68] N. N. Nguyen, A. V. Nguyen, "Nanoreactors" for boosting gas hydrate formation toward energy storage applications, *ACS Nano* 16 (2022) 11504-11515.
- [69] E. J. Beckwée, M. Houleberghs, R-G. Ciocarlan, C. V. Chandran, S. Radhakrishnan, L. Hanssens, P. Cool, J. Martens, E. Breynaert, G. V. Baron, J. F. M. Denayer, Structure

- I methane hydrate confined in C<sub>8</sub>-grafted SBA-15: A highly efficient storage system enabling ultrafast methane loading and unloading, *Appl. Energy* 353 (2024) 122120.
- [70] E. J. Beckwee, G. Watson, M. Houllberghs, D. A. Esteban, S. Bals, P. V. D. Voort, E. Breynaert, J. Martens, G. V. Baron, J. F. M. Denayer, Enabling hydrate-based methane storage under mild operating conditions by periodic mesoporous organosilica nanotubes, *Heliyon* 9 (2023) e17662.
- [71] N. B. Kummamuru, S. W. Verbruggen, S. Lenaerts, P. Perreault, Experimental investigation of methane hydrate formation in the presence of metallic packing, *Fuel* 323 (2022) 124269.
- [72] N. B. Kummamuru, G. Watson, R-G. Ciocarlan, S. W. Verbruggen, P. Cool, P. V. D. Voort, P. Perreault, Accelerated methane storage in clathrate hydrates using mesoporous (Organo-) silica materials, *Fuel* 354 (2023) 129403.
- [73] E. W. Lemmon, M. L. Huber, J. W. Leachman, Revised standardized equation for hydrogen gas densities for fuel consumption applications, *J. Res. Natl. Inst. Stand. Technol.* 113 (2008) 341-350.
- [74] H. P. Veluswamy, P. Linga, Macroscopic kinetics of hydrate formation of mixed hydrates of hydrogen/tetrahydrofuran for hydrogen storage, *Int. J. Hydrogen Energy* 38 (2013) 4587-4596.
- [75] Y. Zhang, G. Bhattacharjee, J. Zheng, P. Linga, Hydrogen storage as clathrate hydrates in the presence of 1,3-dioxolane as a dual-function promoter, *J. Chem. Eng.* 427 (2022) 131771.
- [76] NIST Standard Reference Database, Fundamental physical constants: Avogadro constant, U.S.A.
- [77] T. Kawamura, S. Takeya, M. Ohtake, Y. Yamamoto, Enclathration of hydrogen by organic-compound clathrate hydrates, *Chem. Eng. Sci.* 66 (2011) 2417-2420.
- [78] S. Hashimoto, S. Murayama, T. Sugahara, H. Sato, K. Ohgaki, Thermodynamic and Raman spectroscopic studies on H<sub>2</sub>+tetrahydrofuran+water and H<sub>2</sub>+tetra-n-butyl ammonium bromide+water mixtures containing gas hydrates, *Chem. Eng. Sci.* 61 (2006) 7884-7888.
- [79] R. Ma, H. Zhong, J. Liu, J. Zhong, Y. Yan, J. Zhang, J. Xu, Molecular Insights into Cage Occupancy of Hydrogen Hydrate: A Computational Study, *Processes* 7 (2019) 699.
- [80] H. P. Veluswamy, W. I. Chin, P. Linga, Clathrate hydrates for hydrogen storage: The impact of tetrahydrofuran, tetra-n-butylammonium bromide and cyclopentane as



promoters on the macroscopic kinetics, *Int. J. Hydrogen Energy* 39 (2014) 16234-16243. View Article Online  
DOI: 10.1016/j.ijhydene.2014.05.053

- [81] J.-H. Yoon, J. Han, J. Park, S. Choi, S.-H. Yeon, H. Lee, Spectroscopic identification, thermodynamic stability and molecular composition of hydrogen and 1,4-dioxane binary clathrate hydrate, *J. Phys. Chem. Solids* 69 (2008) 1432-1435.
- [82] H. Yoshioka, M. Ota, Y. Sato, M. Watanabe, H. Inomata, R. L. Smith Jr., Decomposition Kinetics and Recycle of Binary Hydrogen-Tetrahydrofuran Clathrate Hydrate, *AIChE J.* 57 (2011) 265-272.
- [83] Y. Nagai, H. Yoshioka, M. Ota, Y. Sato, H. Inomata, R. L. Smith Jr., C. J. Peters, Binary hydrogen-tetrahydrofuran clathrate hydrate formation kinetics and models, *AIChE J.* 54 (2008) 3007-3016.